

## Effect of Petrolatum Tape Cover on the Hydrogen Permeation of AISI4135 Steel under Marine Splash Zone Conditions

Wenjuan Qu<sup>1,2</sup>, Yanliang Huang<sup>1,\*</sup>, Xiuming Yu<sup>1,2</sup>, Min Zheng<sup>1,2</sup> and Dongzhu Lu<sup>1</sup>

<sup>1</sup> Key Laboratory of Marine Environmental Corrosion and Bio-fouling, Institute of Oceanology, Chinese Academy of Sciences, Qingdao, 266071, China

<sup>2</sup> University of Chinese Academy of Sciences, Beijing, 100049, China

\*E-mail: [hyl@qdio.ac.cn](mailto:hyl@qdio.ac.cn)

Received: 23 April 2015 / Accepted: 15 May 2015 / Published: 27 May 2015

---

Influence of petrolatum tape cover (PTC) technology on the hydrogen permeation behavior of AISI4135 steel has been measured by electrochemical method under simulated splash zone conditions. The hydrogen permeation current of under PTC protection decreased dramatically compared with that without PTC protection. Moreover, the hydrogen permeation current has no significant change when the specimen surface was coated by petrolatum anti-corrosion grease and covered by petrolatum anti-corrosion tape. The PTC technology can provide better protective role for none corroded specimens. The resistances to corrosion were high after prolonged corrosion cycles, when the specimen surfaces were coated by petrolatum anti-corrosion grease and covered by petrolatum anti-corrosion tape.

---

**Keywords:** Hydrogen permeation, petrolatum coating, marine splash zone

### 1. INTRODUCTION

It is well known that the corrosion rate of splash zone is the highest in virtue of sufficient oxygen, sufficient sunshine, salt spray and periodic wetting, etc., in marine environment [1,2]. The anti-corrosion technology of steel structure in splash zone is fairly active with the development of marine oil and gas exploration recently. For instance, Hou *et al.* [3] had studied that thermally sprayed zinc and aluminium coatings can offer high corrosion resistance in splash zone. Li *et al.* [4] researched a solvent-free heavy-duty coating technology which was used extensively in marine structure. Hoar *et al.* reported that Zn-Al alloys and composites around a 50:50 composition were the best coatings from the exposure test result of various alloys and composite coatings in marine and industrial environment for 10.5 years [5]. Studies show that thermally sprayed metal coatings could protect steel in the splash

zone to some extent [6]. However, these protection technologies were not ideal in splash zone. The petrolatum tape cover (PTC) technology is mainly consisting of petrolatum anti-corrosion grease, petrolatum anti-corrosion tape and protective coat. It is the most effective technology to protect steel in splash zone, and it was proved by marine engineering utilizations [7,8]. In addition, the hydrogen entry into high strength steels in marine environment is a significant factor for the susceptibility evaluation of high strength steels to hydrogen embrittlement. Moreover, the susceptibility of high strength steels to hydrogen embrittlement is increased with its strength enhanced, and this restricts the practical application of high strength steels in certain conditions. Therefore, it is essential to study the hydrogen permeation behavior under PTC protection for the safety assessment in marine applications.

The electrochemical hydrogen permeation test [13-15] is a practical technique which allows us to monitor hydrogen entry continuously. This technique was used in this paper to characterize the hydrogen entry into AISI 4135 steel under PTC protection in simulated splash zone conditions. In order to verify the effect of PTC on the hydrogen permeation behavior under splash zone, three different protection procedures were used. Moreover, the electrochemical impedance test was used to evaluate the corrosion resistance under different protection methods.

## 2. EXPERIMENTAL

### 2.1 Materials and specimen

The material used in this paper was an AISI 4135 high strength steel. The chemical compositions are shown in Table 1 and the heat treatment processes are shown in Table 2. For the hydrogen permeation tests, circular plate specimens of 40 mm in diameter and 0.5 mm in thickness were used. Both surfaces of the specimens were polished with emery paper up to # 1000. One side of specimens was plated with Ni in Watt's bath ( $\text{NiSO}_4 \cdot 6\text{H}_2\text{O}$  250 g L<sup>-1</sup>,  $\text{NiCl}_2 \cdot 6\text{H}_2\text{O}$  45 g L<sup>-1</sup>,  $\text{H}_3\text{BO}_3$  40 g L<sup>-1</sup>) at room temperature with a current of 3 mA cm<sup>-2</sup> for 3 min [16]. The estimated thickness of the Ni plating was about 180 nm.

**Table 1.** Chemical compositions of AISI 4135 steel

Element	C	Si	Mn	P	S	Cr	Mo	Ni	Fe
wt%	0.399	0.293	0.509	0.015	0.014	0.903	0.204	0.08	balance

**Table 2.** Heat treatment condition of AISI 4135 steel specimens

Specimen	Heat treatment condition
AISI4135	860 °C thermal insulation 50 min, 370 °C isothermal quenching 30 min, air cooling

## 2.2 Simulation of splash zone conditions

The schematic diagram of the indoor apparatus for the simulation of splash zone conditions is shown in Fig. 1. The electrolytic cell and spray chamber were made by organic glass. The wetting conditions of specimens were simulated by spraying seawater on the surface. The tidal changes and the severity of splash were simulated by adjusting the period of spraying and spraying frequency.

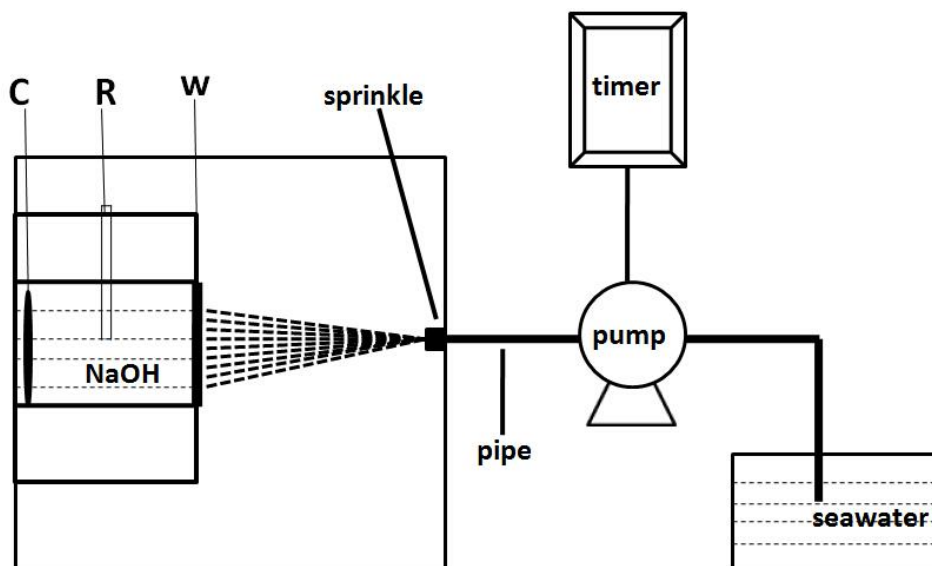


**Figure 1.** Schematic of the indoor apparatus for the simulated splash zone conditions (C: counter electrode, R: reference electrode, W: working electrode)

## 2.3 PTC protection procedures

Petrolatum anti-corrosion grease and petrolatum anti-corrosion tape are the core parts of PTC technology. Three different protection procedures are as follows:

- (1) P1: coating petrolatum anti-corrosion grease on the specimen surface
- (2) P2: coating petrolatum anti-corrosion grease and covering single petrolatum anti-corrosion tape on the specimen surface
- (3) P3: coating petrolatum anti-corrosion grease and covering double petrolatum anti-corrosion tape on the specimen surface

The P1, P2 and P3 are then used to indicate the protection procedures throughout the manuscript.

## 2.4 Hydrogen permeation tests

Hydrogen permeation tests were performed under simulated splash zone conditions as shown in Fig. 1 at room temperature. The double cell which is similar to the Devanathan-Stachurski's cell was used [17]. Three spraying intervals of 1 min, 10min and 30 min were employed to simulate 3 different

severities of seawater splash in this study. As illustrated in Fig. 1, an Hg/HgO electrode and a Pt wire were used as reference and counter electrodes for the hydrogen detection cell. The cell was filled with 0.2 M NaOH solution and the Ni-plated side of specimen was polarized by using a potentiostat at 0.0 mV vs. Hg/HgO electrode for more than 24 h until the residual current lower than  $100 \text{ nA cm}^{-2}$  was reached. Then the hydrogen permeation current was recorded as the specimen subjected to simulated splash zone conditions.

### 2.5 Electrochemical impedance spectroscopy

The experiment was done by using three-electrode system. A SCE and a Pt electrode were used as reference and counter electrodes. Electrochemical impedance spectroscopy (EIS) tests were measured with specimens under seawater film at room temperature. The EIS was performed in a frequency range from  $10^5$  to  $10^{-1}$  Hz.

## 3. RESULTS AND DISCUSSION

### 3.1 Hydrogen permeation currents of unprotected specimen under simulated splash zone conditions

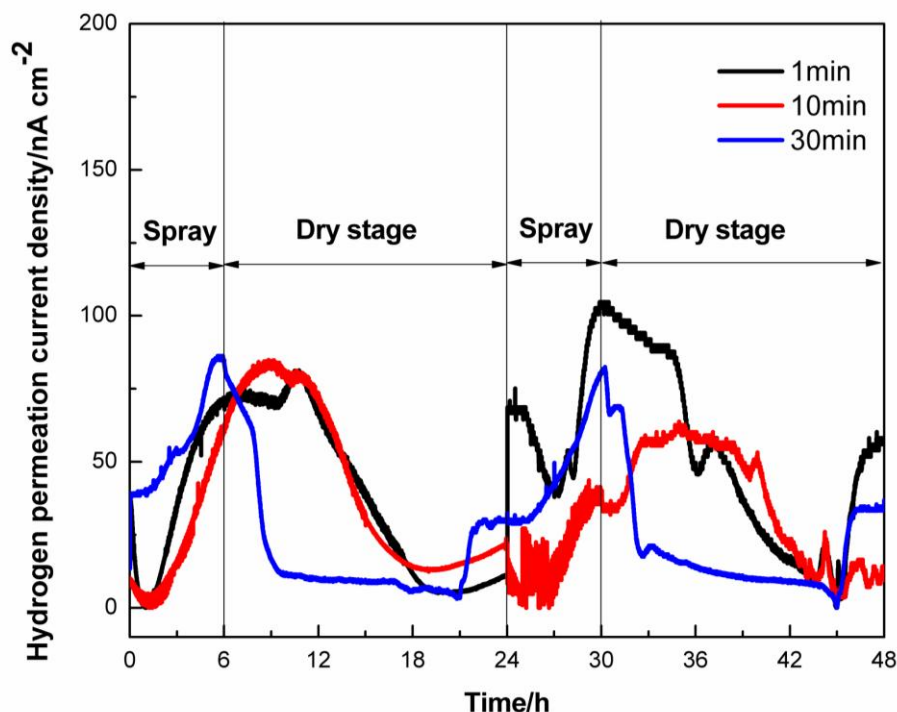


**Figure 2.** Hydrogen permeation currents of unprotected specimen under different spraying interval

The hydrogen permeation currents recorded under spraying interval of 1 min, 10min and 30 min are shown in Fig. 2. Generally, the hydrogen permeation current increased with the increase of spray times. Some minor decrease at the beginning of spray was also observed. As the tide lowered

that was during the dry process, the hydrogen permeation current decreased with time after a peak value was reached. The decrease of hydrogen permeation current at the beginning of spray is mainly because of the pH increase after the spray, since the pH of fresh seawater is around 8. When the specimen was covered by rust layer with the specimen surface was wetted by seawater continuously, the increased concentration of  $H^+$  and high chloride ion would enhance the hydrogen entry as a result of the pH lowering beneath the corrosion product layer [18]. Moreover, the hydrolysis reactions of ferrous ions lead to lowering pH value as well [19].

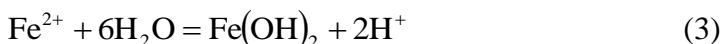
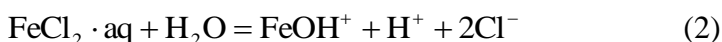


**Table 3.** The amount of hydrogen permeated under different spraying interval within 48h

Specimen	1min	10min	30min
	( $H^+$ /mol)	( $H^+$ /mol)	( $H^+$ /mol)
AISI4135	$3.280 \times 10^{-7}$	$3.265 \times 10^{-7}$	$3.240 \times 10^{-7}$

If we integrate the area below each curve shown in Fig. 2, the amount of hydrogen permeated through specimens can be obtained. The calculated values are shown in Table 3. The effect of seawater spray frequency has little effect on the total amount of permeated hydrogen. This is presumably because of the high humidity at the splash zone. The seawater film formed on the metal surface is slow to be dry. The concentration of dissolved oxygen can be high irrespective of the seawater spraying frequency. The ferrous ions can be further oxidized. In addition, the chloride concentration can also be high. These factors can further lower the pH value and increase the hydrogen entry.



### 3.2 Hydrogen permeation currents of PTC protected specimen under simulated splash zone conditions

Compared Fig. 3 and Fig. 4 with Fig.2, the hydrogen permeation current density decreased dramatically under PTC protections. Under P1 protection, the composite antirust of petrolatum anti-corrosion grease contains an organic compound with polar group and long hydrocarbon chain. Before the rust formed on the metal surface, the protective film can be formed on the specimen interface and blocked the erosion of corrosion medium such as seawater, oxygen and so on by the polar group adsorbing on the metal surface [7]. This protective film reduced the rate of corrosion dramatically. Therefore, the probability of hydrogen permeation is small. Moreover, when the metal surface was covered by rust, the rust transformation agent can react with rust and form ferrum complex. The protective seal layer can be formed on the interface of rust- anticorrosion grease and blocked the further oxidation corrosion.

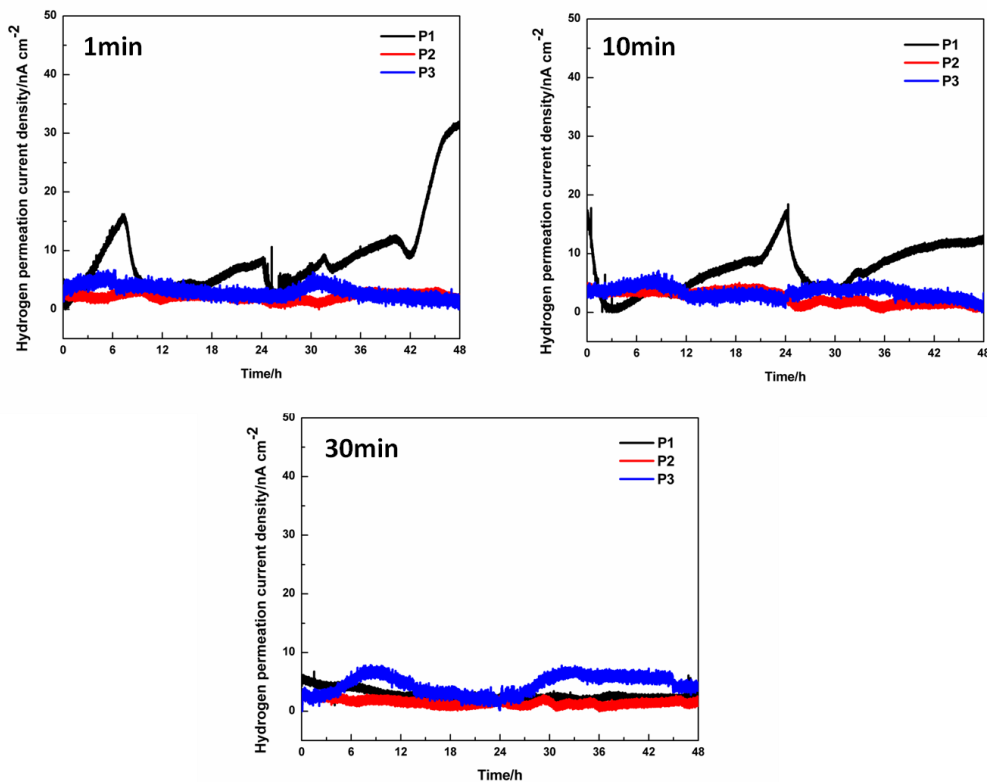


Figure 3. Hydrogen permeation currents of corroded specimen under PTC protection (1min, 10min and 30min are different spraying interval)

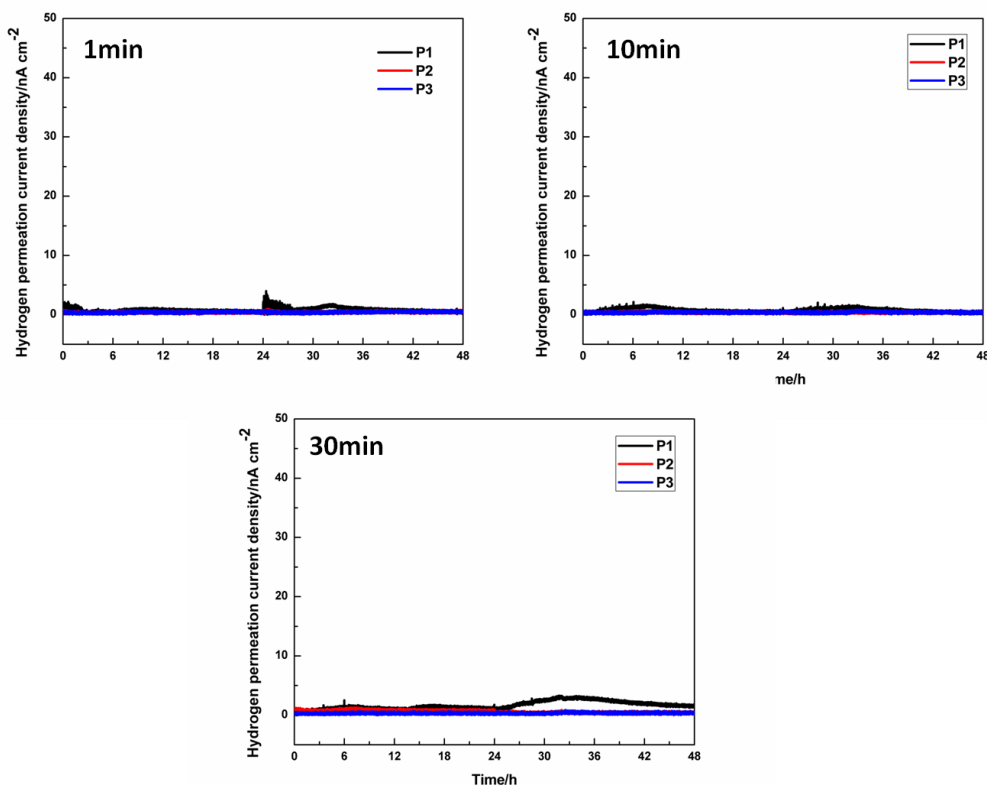


Figure 4. Hydrogen permeation currents of none corroded specimen under PTC protections (1min, 10min and 30min are different spraying interval)

The grease can play double function of derusting and antirust. Furthermore, the rust transformation agent is constituted of tannin and phosphoric acid. Tannin can react with FeOOH of rust layer to form ferric tannates film which is relatively stable on the steel surface [20]. Phosphoric acid can react with rust to form stable phosphate passive film which has protective effect. Moreover, the petrolatum can block the pore with composite antirust and make the adsorbed film more complete [8]. Consequently, the diffusivity of hydrogen became lower, dramatically reducing the hydrogen permeation current density compared with that without PTC protection. But the rust transformation agent could not prevent the corrosion of base metal [21], so the remnant of corrosive species may still present. Therefore, the hydrogen permeation current density of rusty specimen is higher than that of none corroded specimen under P1 protection.

As shown in Fig. 3 and Fig. 4, the hydrogen permeation current has no significant change under P2 and P3 protection. Because of the petrolatum anti-corrosion tapes contain not only the similar anti-corrosion composition to petrolatum anti-corrosion grease but also enhance the sealing property and intensity. In addition, the filler of petrolatum anti-corrosion tape has good chemical stability and mechanical strength. It can provide further protection for petrolatum anti-corrosion grease and base metal. It is difficult for the corrosion medium such as seawater and oxygen entering into the specimen surface. Therefore, the corrosion process became difficult, reducing the possibility of H<sup>+</sup> reduction.

The amount of hydrogen permeated through specimens can be obtained by integrating the area below each curve shown in Fig. 3 and Fig. 4. The calculated values are shown in Table 4. The PTC technology can provide better protective role for none corroded specimen. There is still hydrogen permeated through specimen under PTC protection even the amount of hydrogen permeated is very small. This mainly because the petrolatum anti-corrosion tape is not complete sealed with the experimental apparatus in this study. The seawater can still penetrate into the protective layer. Moreover, the amount of hydrogen permeated increased with the increase of spray times. This was consistent with the experiment results which were obtained by hydrogen permeation tests under no PTC protection.

**Table 4.** The amount of hydrogen permeated under PTC protection within 48 h

Specimen	Rust (H <sup>+</sup> /mol)			No rust (H <sup>+</sup> /mol)		
	1min	10min	30min	1min	10min	30min
Spraying interval						
P1	$7.453 \times 10^{-8}$	$6.233 \times 10^{-8}$	$2.297 \times 10^{-8}$	$1.880 \times 10^{-8}$	$0.855 \times 10^{-8}$	$0.821 \times 10^{-8}$
P2	$2.133 \times 10^{-8}$	$1.866 \times 10^{-8}$	$1.222 \times 10^{-8}$	$0.688 \times 10^{-8}$	$0.474 \times 10^{-8}$	$0.452 \times 10^{-8}$
P3	$1.588 \times 10^{-8}$	$1.536 \times 10^{-8}$	$1.281 \times 10^{-8}$	$0.513 \times 10^{-8}$	$0.453 \times 10^{-8}$	$0.391 \times 10^{-8}$

### 3.3 Electrochemical Impedance Spectroscopy

As shown in Fig. 5, at the initial stage, Nyquist plot is a semi-circle. The Nyquist plots of electrochemical impedance showed an oblique line with the increase of cycles. Moreover, the charge

transfer resistance decreased. It is indicated that the corrosion of specimen was accelerated during wet/dry cycles and the corrosion products couldn't block the occurring of corrosion.

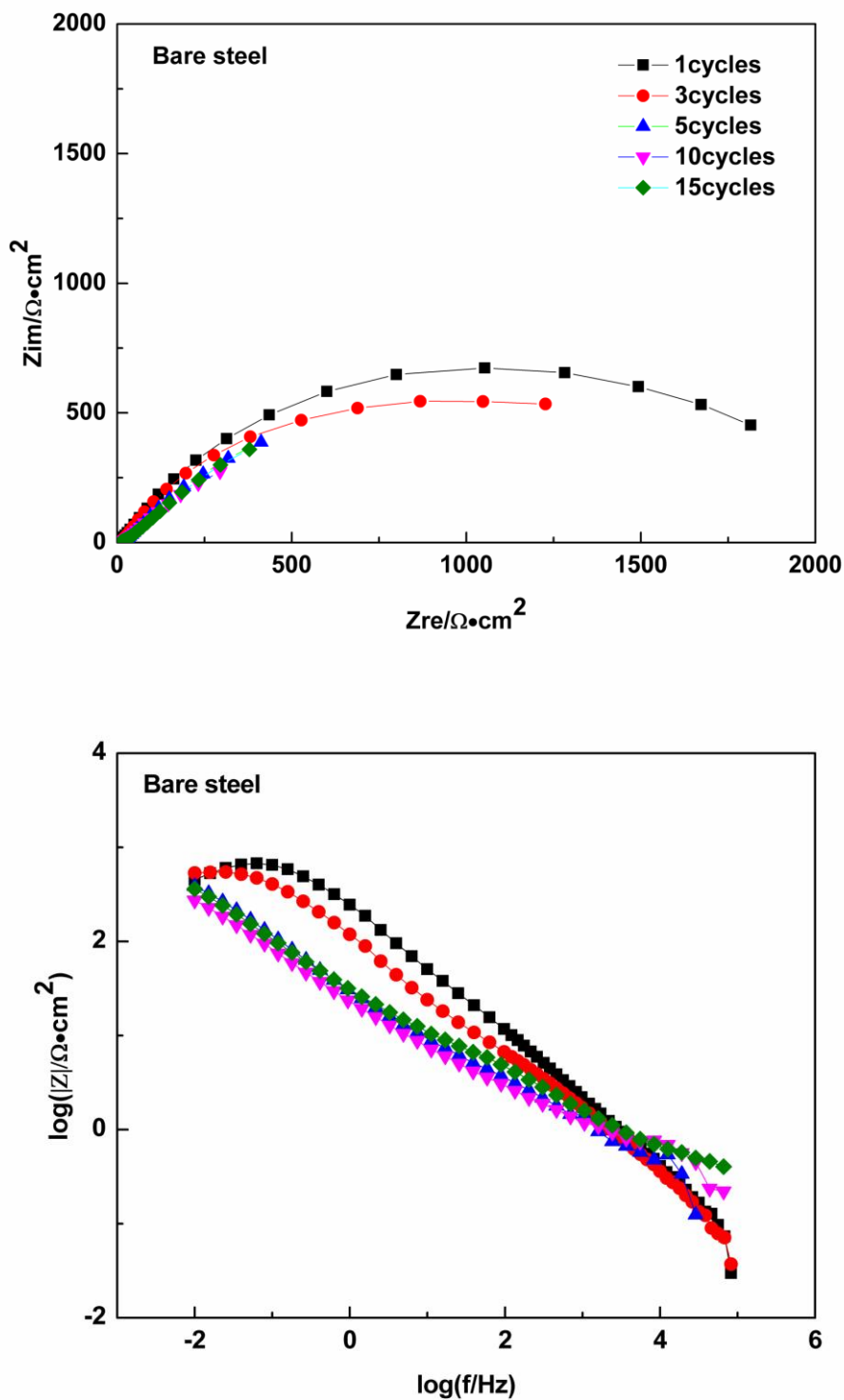


**Figure 5.** The EIS results of specimen under seawater film with no PTC protection after different wet-dry cycles



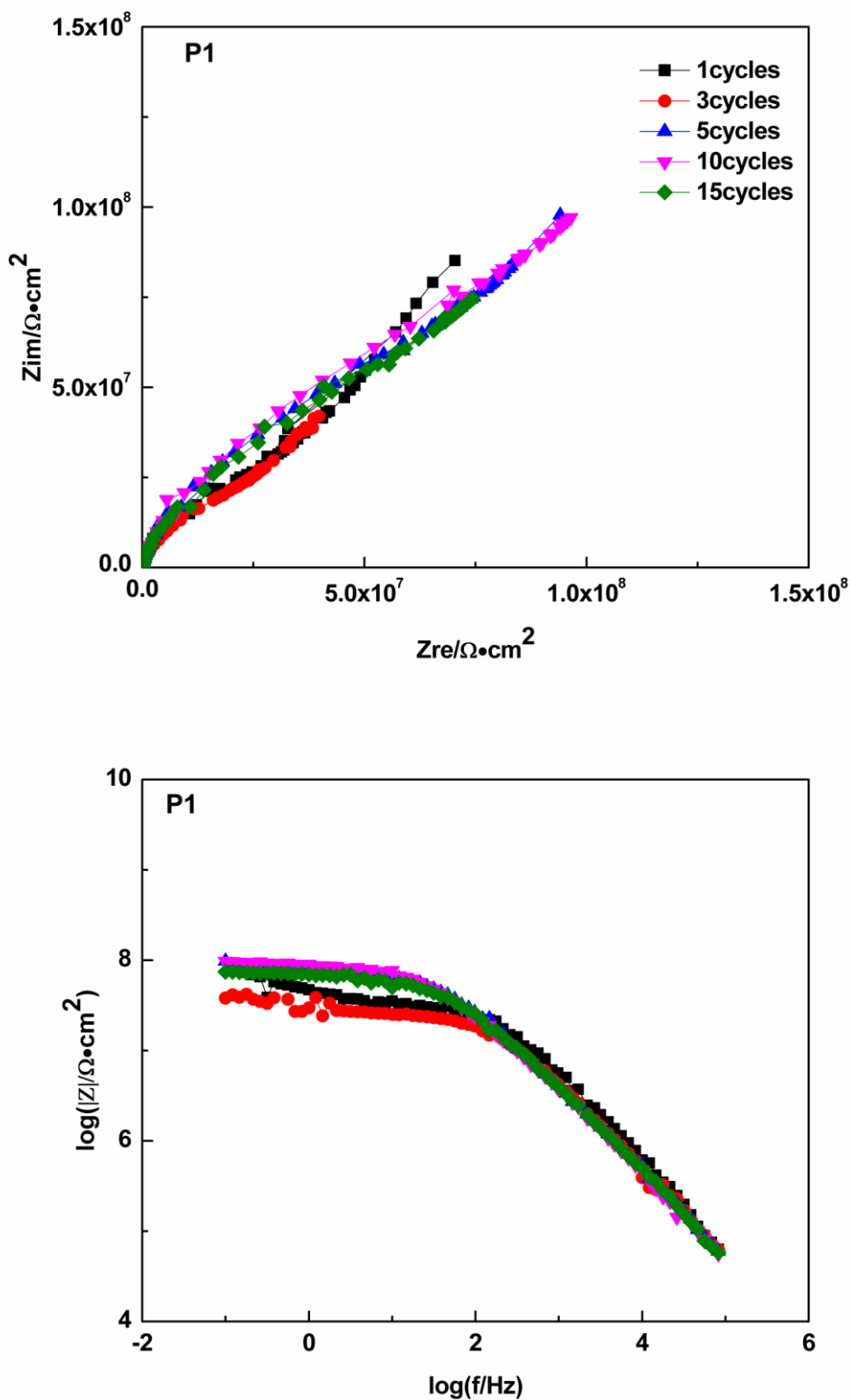


**Figure 6.** The EIS results of specimen under seawater film with P1 protection after different wet-dry cycles

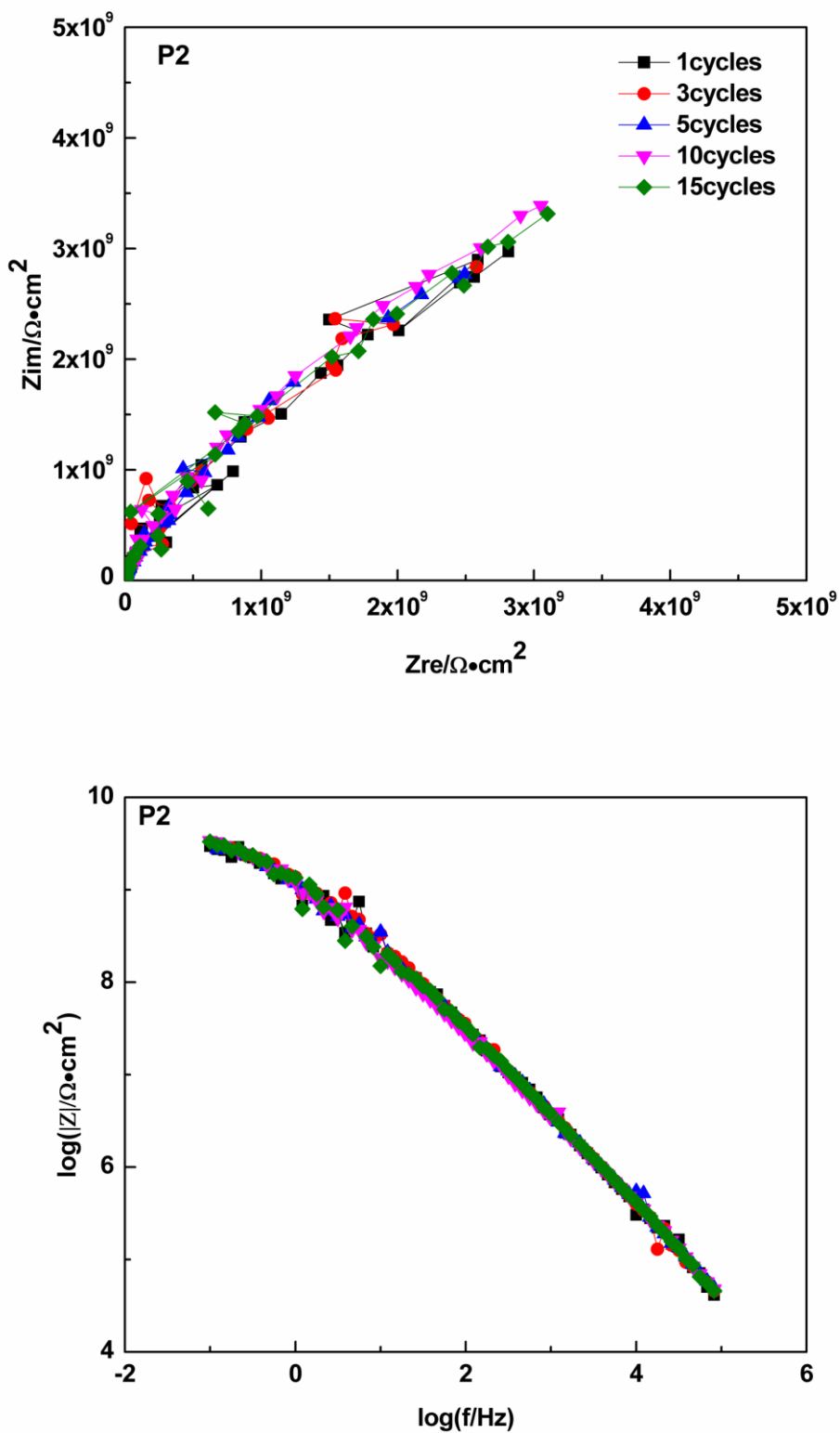


**Figure 7.** The EIS results of specimen under seawater film with P2 protection after different wet-dry cycles

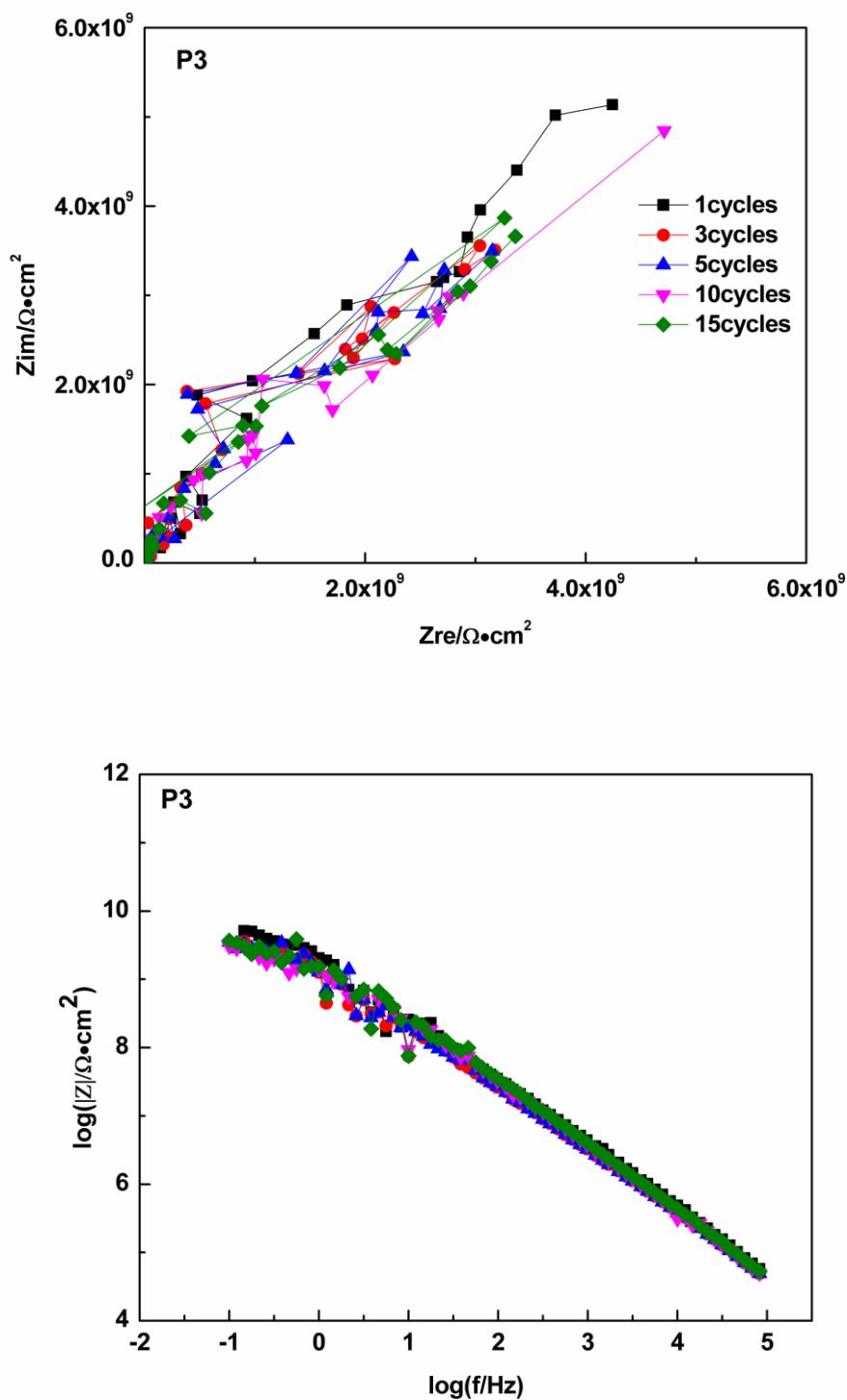


**Figure 8.** The EIS results of specimen under seawater film with P3 protection after different wet-dry cycles

As shown in Fig. 6 – Fig. 8, the plots represent similar patterns after different wet-dry cycles and the impedance spectrum curves overlapped together at high frequency zone as shown in logf-log | Z | plots. But under P1 protection, the resistance was lower than under P2 and P3. The Nyquist plots

showed a capacitive loop in high frequency range and an oblique line in the low frequency range, which may indicated that corrosion medium had diffused to the coating/metal interface. Under P2 and P3 protection, the Nyquist plots of electrochemical impedance showed a single semi-circle with high impedance and plots of  $\log f$ - $\log |Z|$  showed a oblique line. It is indicated that some seawater penetrated into the coating but the anti-corrosion agent is very effective at the coating/metal interface [22]. As a whole, the PTC protection played good anti-corrosion properties after different wet-dry cycles. The PTC protection can not only effectively mitigate the corrosion but also the hydrogen entry under splash zone conditions.

## 5. CONCLUSION

(1) The hydrogen entry into high strength steel occurs during splash zone corrosion conditions, and the effect of seawater spray frequency has little effect on the total amount of permeated hydrogen.

(2) The PTC protection can not only effectively mitigate the corrosion but also the hydrogen entry under splash zone conditions.

## ACKNOWLEDGEMENTS

This work was financially supported by the National Natural Science Foundation of China No.41276087 and Jiangsu Provincial Natural Science Foundation No.BK2012649.

## References

1. M. Smith, C. Bowley and L. Williams, *Mater. Performance*, 41 (2002) 30-33.
2. S. Kuroda, J. Kawakita and M. Takemoto, *Corrosion*, 62 (2006) 635-647.
3. B.R. Hou, J. Zhang, J.Z. Duan, Y. Li and J.L. Zhang, *Corros. Eng., Sci. Technol.*, 38 (2003) 157-160.
4. G.J. Li, L.Y. Liu, S.X. Li, *Coat. Technol. Abstr.*, 35 (2014) 5-10.
5. T.P. Hoar and O. Radovici, *Trans. Inst. Met. Finish.*, 42 (1964) 11-222.
6. W.M. Zhao, Y. Wang, C. Liu, L.X. Dong, H.H. Yu and H. Ai, *Surf. Coat. Technol.*, 205 (2010) 2267-2272.
7. B.R. Hou, *Corrosion and control technology to steel in splash zone*, Science Press Beijing (2011).
8. BR. Hou, *Mater. China*, 33 (2014) 26-30.
9. J. P. Hirth, 1980 Institute of Metals Lecture-the Metallurgical Society of AIME, *Metall. Trans. A*, 11 (1980) 861-890.
10. G. Katano, K. Ueyama and M. Mori., *J. Mater. Sci.*, 36 (2001) 2277-2286.
11. L. W. Tsay, M. Y. Chi, Y. F. Wu, J. K. Wu and D. Y. Lin, *Corros. Sci.*, 48 (2006) 1926-1938.
12. E. Akiyama, K. Matsukado, MQ. Wang and K. Tsuzaki, *Corros. Sci.*, 52 (2010) 2758-2765.
13. M.A.V. Devanathan and Z. Stachurski, W. Beck, *J. Electrochem. Soc.*, 110 (1963) 886.
14. M.A.V. Devanathan and Z. Stachurski, *J. Electrochem. Soc.*, 111 (1964) 619.
15. E. Akiyama, S. Li, T. Shinohara, Z. Zhang and K. Tsuzaki, *Electrochim. Acta*, 56 (2011) 1799-1805.
16. S. Yoshizawa, T. Tsuruta and Y. Yamakawa, *Boushoku-Gijutsu*, 24 (1975) 511-515.
17. M. A. V. Devanathan and Z. Stachurski, *Proc. Roy. Soc. A*, 270A (1962) 90-102.

18. Y. Huang and Y. Zhu, *Corros. Sci.*, 47 (2005) 1545-1554.
19. Q. Yu, Y. L. Huang and C. Zheng, *Corros. Eng., Sci. Technol.*, 43 (2008) 241-247.
20. B. Qian, B.R. Hou and M. Zheng, *Corros. Sci.*, 72 (2013) 1-9.
21. K. Hoffmann and M. Stratmann, *Corros. Sci.*, 34 (1993) 1625-1645.
22. X. Zhao, J. Wang, Y.H. Wang, T. Kong, L. Zhong and W. Zhang, *Electrochem. Commun.*, 9 (2007) 1394-1399.

© 2015 The Authors. Published by ESG ([www.electrochemsci.org](http://www.electrochemsci.org)). This article is an open access article distributed under the terms and conditions of the Creative Commons Attribution license (<http://creativecommons.org/licenses/by/4.0/>).